PH-domain-driven targeting of collybistin but not Cdc42 activation is required for synaptic gephyrin clustering

Suneel Reddy-Alla, Bertram Schmitt, Jörg Birkenfeld, Volker Eulenburg, Sebastien Dutertre, Christian Böhringer, Magdalena Götz, Heinrich Betz, Theofilos Papadopoulos

Angaben zur Veröffentlichung / Publication details:

Reddy-Alla, Suneel, Bertram Schmitt, Jörg Birkenfeld, Volker Eulenburg, Sebastien Dutertre, Christian Böhringer, Magdalena Götz, Heinrich Betz, and Theofilos Papadopoulos. 2010. "PH-domain-driven targeting of collybistin but not Cdc42 activation is required for synaptic gephyrin clustering." *European Journal of Neuroscience* 31 (7): 1173–84. https://doi.org/10.1111/j.1460-9568.2010.07149.x.

PH-Domain-driven targeting of collybistin but not Cdc42 activation is required for synaptic gephyrin clustering

Suneel Reddy-Alla,[1] Bertram Schmitt,[1] Jörg Birkenfeld,[1,*] Volker Eulenburg,[1] Sebastien Dutertre,[1,†] Christian Böhringer,[2] Magdalena Götz,[2,3,4] Heinrich Betz[1] and Theofilos Papadopoulos[1]
[1]Department of Neurochemistry, Max-Planck Institute for Brain Research, 60528 Frankfurt/Main, Germany
[2]Helmholtz Center Munich, German Research Center for Environmental Health, Institute for Stem Cell Research, Neuherberg/Munich, Germany
[3]Physiological Genomics, University of Munich, Munich, Germany
[4]Munich Center for Integrated Protein Science Munich, CIPS(M), Munich, Germany

Abstract

Collybistin (Cb) is a brain-specific guanine nucleotide exchange factor (GEF) that is essential for the synaptic clustering of gephyrin and $GABA_A$ receptors in selected regions of the mammalian central nervous system. It has been previously proposed that Cb regulates gephyrin clustering by activating Cdc42, and thus acts as a signal transducer in a membrane activation process which labels postsynaptic membrane domains for inhibitory synapse formation. Here, we dissected the functional roles of the Dbl-homology (DH) and pleckstrin homology (PH) domains of the constitutively active splice variant Cb II by substituting conserved amino acid residues that are required for GEF activity towards Cdc42 and phosphoinositide binding, respectively. A Cb II mutant lacking any detectable GEF activity towards Cdc42 was still fully active in inducing gephyrin scaffold formation, both in transfected NIH-3T3 cells and in cultured hippocampal neurons. Furthermore, mice with a forebrain-specific inactivation of the Cdc42 gene displayed normal densities of gephyrin and $GABA_A$ receptor clusters in the hippocampus. In contrast, substitution of Cb II PH-domain residues essential for phosphoinositide binding abolished gephyrin recruitment to synaptic sites. Our results provide evidence that the formation of gephyrin scaffolds at inhibitory synapses requires an intact Cb II PH-domain but is Cdc42-independent.

Introduction

The GTP-binding proteins Cdc42, Rho and Rac belong to the Rho subfamily of low-molecular-weight Ras-like GTPases and are at the centre of many fundamental cellular events, such as the establishment of cell polarity, transcriptional regulation, actin cytoskeleton rearrangements, intracellular trafficking and endocytosis (Ridley & Hall, 1992; Hall, 1998). Rho-GTPases activated by guanine nucleotide exchange factors (GEFs) also play key roles in the developing and adult nervous system (Luo, 2000; Yoshizawa *et al.*, 2003). At excitatory synapses, Kalirin-7, the predominant splice form of the multifunctional RhoGEF Kalirin, interacts with the postsynaptic scaffolding protein PSD-95 and has been shown to play an essential role in synaptic morphology and function including cognitive processes (Penzes *et al.*, 2001; Ma *et al.*, 2008a,b). At inhibitory synapses, gephyrin, a scaffolding protein which anchors glycine receptors (GlyRs) and γ-aminobutyric acid receptors ($GABA_A$Rs) to the postsynaptic cytoskeleton (reviewed in Kneussel & Betz, 2000; Fritschy *et al.*, 2008), interacts with the RhoGEF collybistin (Cb) (Kins *et al.*, 2000). Ablation of Cb expression by conventional or conditional gene inactivation in mice indicates that Cb is essential for both the formation and maintenance of gephyrin and gephyrin-dependent $GABA_A$R clusters at inhibitory postsynaptic sites in selected regions of the mammalian forebrain (Papadopoulos *et al.*, 2007, 2008).

The molecular mechanisms through which Cb specifies the formation and stabilization of inhibitory postsynapses are not fully understood. Due to the presence of tandem Dbl-homology (DH) and pleckstrin homology (PH) domains, Cb has been classified as a Dbl-like GEF for Rho-GTPases (Kins *et al.*, 2000). Cb exists in multiple splice variants (I–III) (Kins *et al.*, 2000; Harvey *et al.*, 2004), and its human homologue, hPEM-2, has been shown to function as a GEF specific for Cdc42 (Reid *et al.*, 1999). More recently, the crystal structure of the Cdc42–Cb II [the shorter splice variant of Cb lacking the N-terminally located Src homology 3 (SH3)-domain] complex has been determined (Xiang *et al.*, 2006). This study demonstrated that Cb II catalyses nucleotide exchange on Cdc42 more efficiently than the prevailing splice variant Cb I, which contains an additional SH3-domain. Hence, it is thought that similar to what is known for the homologous GEFs Asef 1 and 2 (Hamann *et al.*, 2007; Mitin *et al.*,

Correspondence: Dr H. Betz or Dr T. Papadopoulos, as above.
E-mail: Neurochemie@mpih-frankfurt.mpg.de or Papadopoulos@mpih-frankfurt.mpg.de

**Present address*: Bayer Schering Pharma AG, Nattermannallee 1, 50829 Koeln, Germany.

†*Present address*: Atheris Laboratories, CH-1233 Bernex, Geneva, Switzerland.

2007), the SH3-domain acts as an auto-inhibitory domain retaining Cb I in an inactive conformation. Consistent with this view, coexpression of Cb II, but not Cb I, with gephyrin in human embryonic kidney (HEK) 293 cells alters the subcellular distribution of gephyrin by relocating it from large intracellular aggregates into small clusters at the plasma membrane (Kins *et al.*, 2000). However, in transfected cortical neurons both the SH3-containing and the SH3-lacking splice variants of Cb similarly redistribute gephyrin into synaptic clusters (Harvey *et al.*, 2004). This suggested that in specific neuronal subpopulations Cb I is locally 'activated' by an SH3-interacting ligand or 'trigger' protein. Indeed, in a recent study neuroligin 2 (NL2) was shown to interact with the SH3-domain of Cb and to induce Cb-dependent gephyrin clustering in a neuron-specific manner by relieving SH3-mediated inhibition (Poulopoulos *et al.*, 2009). NL2 is a member of the neuroligin family of postsynaptic cell adhesion proteins (Chih *et al.*, 2005; Craig & Kang, 2007; Jamain *et al.*, 2008) that colocalizes with gephyrin at inhibitory synapses (Varoqueaux *et al.*, 2004). The recruitment of NL2 under GABAergic and glycinergic presynaptic terminals is thought to create nucleation sites for gephyrin deposition and receptor clustering and thereby to induce postsynaptic membrane differentiation. This is proposed to require the activation of Cb through a mechanism involving NL2–Cb and NL2–gephyrin interactions (Poulopoulos *et al.*, 2009). According to these data and a previously proposed model, NL2-bound Cb may trigger the deposition of gephyrin by activating Cdc42, a candidate downstream effector, in a membrane activation process that labels postsynaptic membrane domains for inhibitory synapse formation (Kins *et al.*, 2000; Kneussel & Betz, 2000).

Here we address the question of whether the activation of Cdc42 is required for inhibitory synapse formation by using the constitutively active splice variant II of Cb. Based on the known three-dimensional structure of Cb II and other GEFs of the Dbl family, we replaced amino acid residues within the DH-domain of Cb II in order to identify sites involved in its catalytic activity towards Cdc42. This revealed that residues NE232–233 of Cb II are essential for Cdc42 activation. In the Cb II NE232–233AA double mutant, both the ability to activate Cdc42 upon coexpression and to induce the formation of filopodia, a hallmark of Cdc42 activation, were completely lost. However, the NE232–233AA substitution did not impair gephyrin recruitment into submembraneous clusters in both NIH 3T3 cells and dissociated hippocampal neurons. Furthermore, conditional inactivation of Cdc42 in the mouse forebrain at early developmental stages did not affect the clustering of gephyrin and $GABA_A$Rs at developing inhibitory synapses. Thus, the GEF activity of Cb towards Cdc42 is not required for postsynaptic membrane activation as suggested previously (Kneussel & Betz, 2000; Xiang *et al.*, 2006). Notably, replacement of two adjacent arginine residues (R303/R304) that are required for the binding of phosphatidylinositol-3-phosphate (PI3P) to the $\beta3/\beta4$ loop of the PH-domain abolished the ability of Cb II to localize gephyrin to inhibitory postsynaptic sites. These data indicate that phosphoinositide binding of Cb but not Cdc42 activation is required for synaptic gephyrin clustering.

Materials and methods

Mutant mice

The generation of $Emx1^{Cre/Cdc42\Delta ex2fl/fl}$ mice has been described previously (Cappello *et al.*, 2006). Homozygous C57Bl/6J//129/Sv-Cdc42fl/fl possessing loxP sites flanking exon 2 of the murine Cdc42 gene (Wu *et al.*, 2006) were crossed with $Emx1^{Cre/Cdc42\Delta ex2fl/+}$ mice to obtain the Cdc42 mutants $Emx1^{Cre/Cdc42\Delta ex2fl/fl}$. Phenotypically normal mice containing only one loxP-flanked ('floxed') allele and no Cre transgene derived from the same litters were used as controls. Genotyping was performed by PCR as described (Cappello *et al.*, 2006).

Antibodies

The following antibodies were used for immunostaining and/or Western blotting: monoclonal antibody specific for gephyrin (mouse; mAb7a; 1 : 400); antibody against the $\gamma2$ subunit of $GABA_A$ receptors (guinea-pig; 1 : 4000; kindly provided by Dr Jean-Marc Fritschy, University of Zurich, Switzerland); antibody against the vesicular inhibitory amino acid transporter (VIAAT; affinity-purified polyclonal rabbit; Synaptic Systems, Goettingen, Germany; 1 : 500); anti-HA (mouse monoclonal; clone HA-7; Sigma, Taufkirchen, Germany; 1 : 1000), anti-Myc (rabbit polyclonal; ab9106; Abcam, Cambridge, UK; 1 : 5000, for Western blotting); and anti-Myc (rabbit polyclonal; Roche, Heidelberg, Germany; 1 : 300, for immunocytochemistry). Alexa Fluor-633 phalloidin and secondary antibodies (guinea-pig, rabbit or mouse, Alexa-488, Alexa-546 or Alexa-635 conjugated for immunostaining) were from Invitrogen (Karlsruhe, Germany). Horseradish peroxidase-conjugated secondary antibodies for Western blotting were from Promega (Madison, WI, USA).

cDNA constructs

The construction of C-terminally haemagglutinin (HA)-tagged Cb I and Cb II has been described previously (Kins *et al.*, 2000). For the generation of pCIS-Cb II-ΔDH, a *Kpn*I/*Bgl*II fragment was deleted from pCIS-Cb II (Kins *et al.*, 2000). The Cb I, Cb II and Cb II-ΔDH cDNAs, including the HA-tag, were transferred from pCIS2 into the pEGFP-N2 vector (BD, Heidelberg, Germany) using *EcoR*I and *Not*I cleavage sites, thereby removing the EGFP sequence. The Cb II point mutants were generated in p(EGFP)Cb II-HA by oligonucleotide-directed mutagenesis with the QuickChange mutagenesis kit (Stratagene, Amsterdam, Netherlands) according to the manufacturer's instructions. The sequences of mutagenized cDNAs were confirmed by automated DNA sequencing.

The pEGFP-C2-gephyrin plasmid has been previously described (Fuhrmann *et al.*, 2002). The pRK5Myc-Cdc42 construct was obtained from Addgene Inc. (Cambridge, MA, USA). The following N-terminally 3× HA-tagged constructs were obtained from the Guthrie cDNA Resource Center (Sayre, PA, USA): Cdc42 G12V, Cdc42 T17N, Rac1 G12V, RhoA G14V. The plasmid pRK5Myc-Cdc42BD encoding the Cdc42 binding domain of Wiskott–Aldrich syndrome protein (WASP) was a generous gift of Dr Alan Hall (London, UK).

Cell culture and transient expression of recombinant proteins in HEK 293 and NIH-3T3 cells

HEK 293 cells (ATCC, Manassas, USA, #CRL-1573) were plated onto 10-cm tissue culture dishes containing Dulbecco's modified Eagle's medium (DMEM; Invitrogen) supplemented with 2 mM L-glutamine, 10% (v/v) fetal calf serum (FCS), 50 U/mL penicillin and 50 U/mL streptomycin, and incubated at 37°C in 5% CO_2. After reaching 90–95% confluence, cells were washed once with DMEM without supplements and incubated in 4.5 mL DMEM (antibiotics- and serum-free). Cells were transfected using Lipofectamine 2000 (Invitrogen) according to the manufacturer's protocol. Briefly, 3 μg of Cb II cDNA or control plasmid (pEGFP-N2 vector), 0.8 μg of Myc-Cdc42 cDNA and 10 μL Lipofectamine 2000 reagent were used per

transfection. After 4 h, culture dishes with transfected cells were supplemented with 10 mL of DMEM containing serum and antibiotics, and further incubated for an additional 20 h at 37°C and 5% CO_2.

NIH-3T3 cells (ATCC, Manassas, USA, # CRL-1658) were transfected using the Nucleofector solution R (Lonza, Koeln, Germany) according to the manufacturer's instructions. Cultured cells were trypsinized, pelleted and resuspended at a density of 10^6 cells per nucleofection sample. Cells were transfected with 3 μg of total DNA using equal amounts of the respective plasmids and empty vector DNA. Electroporated cells were plated onto fibronectin-coated coverslips in 24-well plates and maintained for 6 h in 0.5 mL supplemented DMEM at 37°C in 5% CO_2. Cells were washed with and maintained for an additional 18 h in 0.5 mL serum-free DMEM supplemented as above.

In vivo *Cdc42 activation assay*

The glutathione-sepharose immobilized GST-PAK1 PBD, a glutathione-S-transferase (GST) fusion-protein containing the p21-binding domain (PBD, residues 67–150) of human PAK-1, was purchased from Cytoskeleton (PAK02; Tebu-bio, Frankfurt, Germany). HEK 293 cells were grown and transfected as described above using 0.8 μg of Myc-Cdc42 cDNA with or without 3 μg of the different Cb II-HA constructs. Twenty-four hours after transfection, cells were washed twice with ice-cold phosphate-buffered saline (PBS) and lysed on the dish for 20 min by adding 0.8 mL of lysis buffer [25 mM HEPES, pH 7.5, 150 mM NaCl, 1% (w/v) Igepal CA-630, 2% (v/v) glycerol, 25 mM NaF, 10 mM $MgCl_2$, 1 mM EDTA, 1 mM sodium orthovanadate, 10 μg/mL leupeptin, 10 μg/mL aprotinin]. After centrifugation at 14 000 ***g*** for 10 min at 4°C, the supernatants of the lysates were incubated at 4°C for 1 h with 15 μg of GST-PAK1 PBD under constant agitation. The beads were washed four times with lysis buffer, and the amounts of total and bound recombinant Myc-Cdc42 were detected by Western blotting with an antibody against the Myc epitope tag. Western blotting was performed as described (Papadopoulos *et al.*, 2007).

Transfection of cultured hippocampal neurons

The mother was deeply anesthetized using isofluran (DeltaSelect, Dreieich, Germany) killed by cervical dislocation and decapitated. Embryos were removed and decapitated. Hippocampal neurons were isolated from embryonic day (E)18 rat embryos (Wistar) and cultivated as described previously (Fuhrmann *et al.*, 2002). At day 10 *in vitro*, neurons were transfected using Lipofectamine 2000 (Invitrogen) as described (Armsen *et al.*, 2007).

Immunocytochemistry

Cells were washed twice with PBS containing 0.9 mM $CaCl_2$ and 0.5 mM $MgCl_2$, fixed for 10 min with PBS containing 4% (w/v) paraformaldehyde, washed once with PBS, permeabilized for 30 min in PBS containing 0.1% (v/v) Triton X-100 and 1% (w/v) bovine serum albumin (BSA), and then blocked for 1 h with PBS containing 1% BSA (PBS/BSA). Fixed cells were incubated for 1.5 h with primary antibodies, washed twice in PBS/BSA for 5 min and incubated for 1 h with fluorescently labelled secondary antibodies (Alexa-488, Alexa-546 and Alexa-635; Invitrogen) at 1 : 1000 dilution in PBS/BSA. To visualize actin filaments, cells were stained for 1 h with Alexa Fluor-633 phalloidin (Invitrogen) diluted 1 : 100 in PBS/BSA. After washing three times for 5 min in PBS, cells were counterstained with DAPI for 5 min, rinsed in PBS and coverslipped with Aqua Poly/Mount (Polysciences, Inc., Eppelheim, Germany). Neuronal viability as assessed by DAPI staining (Jiang *et al.*, 2000) was unaffected in all cultures selected for imaging and quantification (data not shown). Images were collected with a Leica TCS-SP confocal laser scanning microscope (Leica Microsystems, Mannheim, Germany) as described (Bausen *et al.*, 2006).

Dendritic clusters of VIAAT, recombinant gephyrin or Cb II immunoreactivity were counted over a dendrite length of 30 μm and compared for colocalization. For each Cb II construct (Cb II WT, Cb II-NE232–233AA and Cb II-RR303–304NN), three distinct transfections of identically processed cultures were analysed, and five images were collected from randomly selected dendrites of five individual neurons per transfection experiment. Data are expressed as means ± SEM. Statistical significance was evaluated with Student's *t*-test.

Immunohistochemistry

Immunostainings were performed in parallel for all sections prepared from brains of three independent litters including $Emx1^{Cre/Cdc42\Delta ex2fl/fl}$ adult mice and their phenotypic wild-type (WT) ($Emx1^{Cre(-)/Cdc42\Delta ex2fl/+}$) littermates. Mice were deeply anaesthetized using isofluran (DeltaSelect, Dreieich, Germany). Animals were killed by cervical dislocation and decapitated. Brains were immediately removed and frozen on dry ice. Coronal hippocampal cryostat sections (14 μm) were fixed with 4% (w/v) paraformaldehyde in PBS for 10 min at 4°C, washed twice for 2 min in PBS and once with SC buffer [10 mM sodium citrate, 0.05% (v/v) Tween-20, pH 8.0]. Sections were immersed in a pre-heated staining dish containing SC buffer and incubated for 30 min at 95°C. After allowing the slides to cool at room temperature for 20 min, sections were rinsed twice for 2 min in PBS, permeabilized with 0.3% (w/v) Triton X-100, 4% (v/v) goat serum in PBS, blocked for 3 h with 10% goat serum in PBS, and incubated overnight at 4°C with primary antibodies at appropriate dilutions in PBS/10% goat serum. Sections were then rinsed three times for 5 min in PBS and incubated for 1 h at room temperature with secondary antibodies (Alexa-488 and Alexa-546; Invitrogen; 1 : 1000 in PBS/3% goat serum). After washing three times for 5 min in PBS, the sections were counterstained with DAPI and mounted as described above. Serial confocal images were captured at a total magnification of either 400× or 630× on the Leica TCS-SP confocal laser-scanning microscope. Three-dimensional overlaid images were compressed using a maximum projection algorithm provided with the Leica TCS software. The numbers of gephyrin and $GABA_AR$ γ2-subunit immunoreactive puncta were counted per 500 μm^2. For each genotype, three distinct brain preparations were analysed, and four randomly selected image areas were used for quantifications.

Sections adjacent to those used for immunohistochemical analysis were stained with cresyl-violet using standard procedures. Images of cresyl-violet-stained slices were captured at a total magnification of either 50× or 400× on an Axiophot microscope (Carl Zeiss, Göttingen, Germany).

Results

Conserved residues within the DH-domain that are required for GEF activity of Cb II

X-ray analysis of GEF-Rho protein complexes (Aghazadeh *et al.*, 1998; Liu *et al.*, 1998; Worthylake *et al.*, 2000; Rossman *et al.*, 2002; Snyder *et al.*, 2002) and the functional characterization of point mutations in several Dbl family members (Zhu *et al.*, 2000; Debreceni

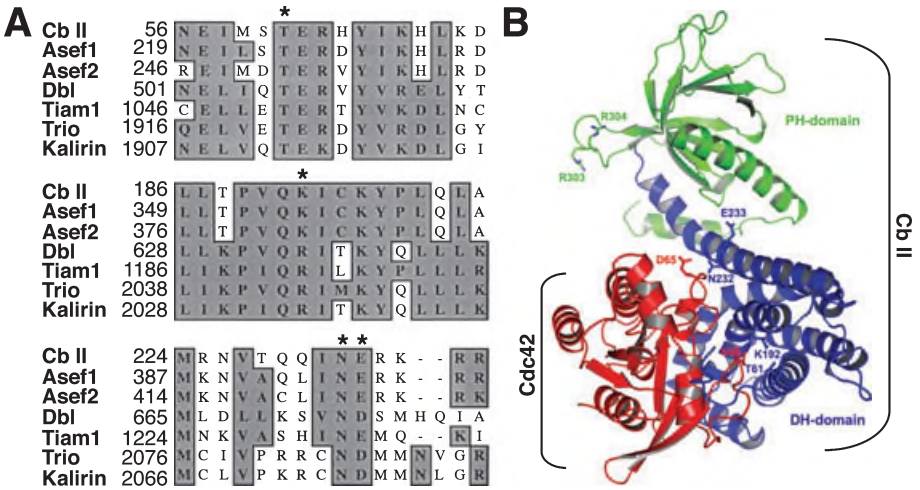

FIG. 1. Highly conserved residues in the DH-domain of Cb II. (A) Amino acid alignment of DH-domain sequences of Cb II, Asef1, Asef2, Dbl, Tiam1, Trio and Kalirin. Highly conserved residues are boxed. Residues that are mutated to alanine in the current study are indicated by an asterisk. (B) Three-dimensional structure of the Cb II–Cdc42 protein complex according to Xiang *et al.* (2006) (pdb code: 2DFK). Side chains in the DH-domain (blue) and the PH-domain (green) that were mutated in the current study are indicated. V36 and D65 of Cdc42 (red) are predicted to interact with the side chains T61 and N232 of Cb II, respectively.

et al., 2004; Schiller *et al.*, 2005) have identified conserved amino acid residues within the DH-domain that are required for GEF activity. Based on the crystal structure of the Cb II–Cdc42 complex and structural mapping data (Xiang *et al.*, 2006), we replaced the following conserved DH-domain residues of Cb II by alanines: T61, K192 and NE232–233, which correspond to T506, R634 and ND673-674 of Dbl, respectively. These side chains are particularly well conserved among Dbl family members (Fig. 1A; Zhu *et al.*, 2000), and their functional roles in GTP-loading are well understood. T61 of Cb II is involved in a critical van der Waals interaction with the switch I residue V36 of Cdc42 in the Cb II–Cdc42 complex (Fig. 1B; Xiang *et al.*, 2006). A similar van der Waals pairing is also seen in the other available structures of GEF-Rho protein complexes, and mutation of the corresponding residues T506 of Dbl and T1244 of Trio has been shown to result in complete or partial inactivation of Rho-GEF activity (Zhu *et al.*, 2000; Debreceni *et al.*, 2004). Mutation of R634 in Dbl, the residue homologous to K192 in Cb II, led to a strong reduction of nucleotide exchange activity towards Cdc42, which could be attributed to a possible disruption of DH-domain tertiary structure (Zhu *et al.*, 2000). N232 of Cb II forms a hydrogen bond with the conserved D65 residue of Cdc42 (Fig. 1B; Xiang *et al.*, 2006). Again, this hydrogen bond is highly conserved among all Dbl family GEF-Rho-GTPase complexes, and double mutations of the corresponding asparagine residue and the adjacent acidic (E or D) residue in several Dbl family GEFs have been found to cause a complete loss of exchange activity (Zhu *et al.*, 2000; Debreceni *et al.*, 2004; Schiller *et al.*, 2005).

To examine whether the Cb II mutants T61A, K192A and NE232–233AA activate Cdc42 *in vivo*, we cotransfected HA-tagged mutant and WT Cb constructs with Myc-tagged Cdc42 into HEK 293 cells. Expression of HA-Cb II proteins and Myc-Cdc42 was confirmed by Western blotting of the cell lysates with anti-HA and anti-Myc antibodies (Fig. 2A). The amount of activated Myc-Cdc42 was determined by binding to immobilized PAK1-PBD, an activation state-specific probe that associates specifically with Cdc42-GTP but not with Cdc42-GDP (Manser *et al.*, 1994). *In vitro* loading of Myc-Cdc42 in HEK293 cell lysates with an excess of non-hydrolyzable GTPγS produced markedly increased amounts of the small GTPase in GST-PAK1-PBD co-precipitates as compared with those isolated in the presence of excess GDPβS (Supporting information, Fig. S1). This confirms that GST-PAK1-PBD is a useful probe for monitoring the activation state of Cdc42. Also, immobilized GST-PAK1-PBD bound significantly more Myc-Cdc42-GTP in extracts prepared from WT Cb II-coexpressing cells as compared with those from cells expressing Myc-Cdc42 alone (Fig. 2A and supporting Fig. S1). Apparently, our effector pull-down assay was effective in detecting the GEF activity of Cb II upon heterologous expression. Notably, when the Cb II mutants T61A, K192A and NE232–233AA were coexpressed with Myc-Cdc42, the GST-PAK1-PBD pull-down revealed strongly reduced catalytic activations as compared with WT Cb II in four independent experiments (Fig. 2A, and data not shown). Densitometric scanning of the relative band intensities of the bound Myc-Cdc42-GTP immunoreactivity revealed values of 23.2 ± 5.0, 13.8 ± 5.0 and 6.7 ± 4.4% (mean ± SEM) for mutants T61A, K192A and NE232–233AA, respectively, as compared with that obtained with WT Cb II (Fig. 2B). From extracts of cells expressing Myc-Cdc42 alone, immobilized GST-PAK1-PBD bound 9.3 ± 13.1% (mean ± SD) of the amount of Myc-Cdc42-GTP that could be precipitated from extracts of WT Cb II-coexpressing cells (Fig. 2B). These results indicate that the NE232–233AA mutant of Cb II had completely lost its GEF activity, as the levels of Cdc42 activation obtained with this mutant were even lower than those found with cells expressing Myc-Cdc42 alone. In agreement with previous studies on other GEFs (Zhu *et al.*, 2000; Debreceni *et al.*, 2004), the T61A and K192A mutants showed strong reductions in their Cdc42 activation potential. In the K192A mutant, residual activity was not significantly higher than in control cells transfected with Myc-Cdc42 only.

GEF activity of Cb is essential for Cdc42-induced filopodia formation in 3T3 cells

It has been previously established that Cdc42 activation is critical for filopodia formation in different cell lines; in contrast, Rac1 activation participates in membrane ruffling and lamellipodia formation, whereas RhoA activity is essential for actin stress fibre formation in NIH-3T3 and other cells (Ridley & Hall, 1992; Nobes & Hall, 1995; Hall, 1998). To monitor GTPase-induced actin rearrangements, we transfected constitutively active forms of these

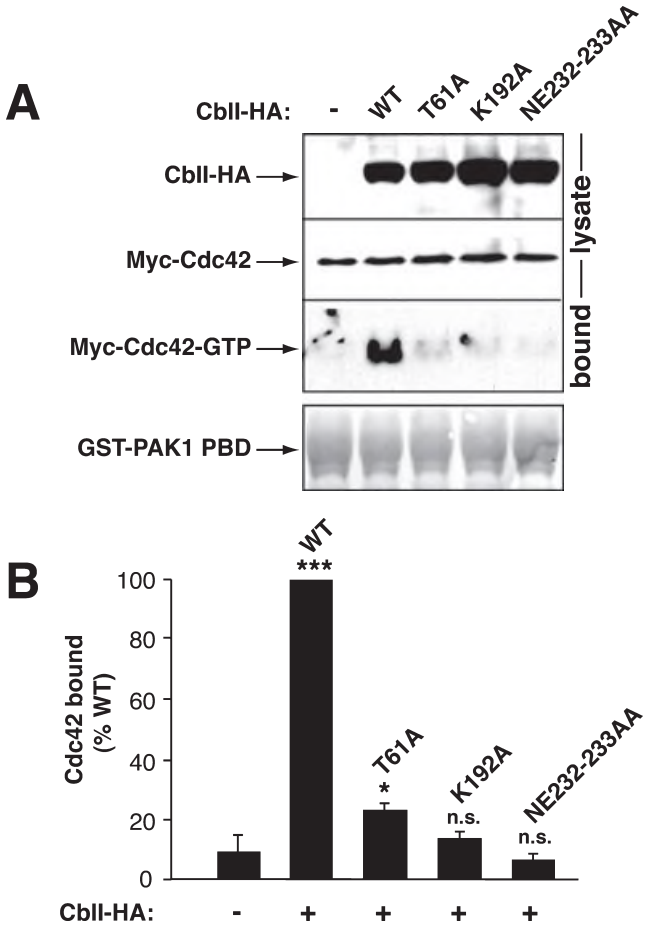

FIG. 2. Activation of Cdc42 by Cb II and the DH-domain mutants thereof. (A) Myc-tagged Cdc42 was transfected either alone (−) or cotransfected with HA-tagged Cb II WT or the individual DH-domain mutants into HEK 293 cells. Twenty-four hours after transfection, cell lysates were used for GST-PAK1 PBD affinity precipitation. Coprecipitated GTP-bound Cdc42 was detected by Western blotting with anti-Myc antibody. To monitor Cdc42 and Cb II expression, 2% of the cell lysates used for GST-PAK1 PBD binding assays were in addition subjected to anti-Myc and anti-HA blotting. Ponceau-staining (bottom panel) was used to confirm that equal amounts of GST-PAK1 PBD were added to each incubation. (B) Relative band intensities (% WT) of coprecipitated Cdc42. Results represent mean ± SEM from four independent experiments using proteins from different preparations (*$P < 0.05$; ***$P < 0.001$; ns: not significant; unpaired, two-tailed Student's *t*-test; $n = 4$).

Rho GTPases (Cdc42-G12V, Rac1-G12V and RhoA-G14V) in NIH-3T3 fibroblasts by nucleofection (> 80% transfection efficiency), serum-starved the cells for 18 h, fixed them and analysed their morphology by confocal microscopy (supporting Fig. S2). Under the experimental conditions used (see Materials and methods), this reproduced the morphological effects induced by activated Cdc42, Rac1 and RhoA described previously (Nobes & Hall, 1995). We then expressed eGFP, Cb I (the SH3-containing splice variant of Cb) and Cb II in NIH-3T3 cells under the same experimental conditions (supporting Fig. S3). Both Cb splice variants caused the formation of filopodia indicative of Cdc42 activation, whereas GFP alone did not induce any actin phenotype (supporting Fig. S3A–C). Notably, deletion of the DH-domain abolished Cb II-induced filopodia extensions and actin rearangements (supporting Fig. S3D). To reveal whether Cdc42 has to be activated for Cb II-induced filopodia formation, we coexpressed the Cdc42-binding domain of the WASP (Aspenstrom *et al.*, 1996; Kolluri *et al.*, 1996). This domain interacts specifically with the GTP-bound form of Cdc42 family members and thereby interferes with Cdc42-mediated signal transduction (Symons *et al.*, 1996). Coexpression of this construct prevented the formation of Cb II-induced filopodia (supporting Fig. S3E). These results indicate that Cb induces the formation of filopodia via direct activation of Cdc42.

To further characterize the T61A, K192A and NE232–233AA mutants, we examined their effects on cell morphology and actin cytoskeleton rearrangement in NIH-3T3 fibroblasts under the conditions described above. HA-tagged WT Cb II and the T61A, K192A and NE232–233AA mutants, as well as eGFP (not shown), were expressed, and transfected cells were analysed for the presence of filopodia (Fig. 3A–D). F-actin staining of the cells revealed that under serum-free conditions WT Cb II as well as the T61A and, to a lesser extent, K192A mutants induced filopodial structures. In contrast, the NE232–233AA mutant completely failed to induce filopodia and caused changes in the actin cytoskeleton similar to those observed with the DH deletion mutant of Cb II (Fig. 3A–D and supporting Fig. S3D). The proportion of transfected cells producing filopodia was 3.2 ± 1.1, 30.0 ± 1.8, 26.7 ± 2.0, 10.8 ± 1.4 and 4.0 ± 1.0% for eGFP-, WT Cb II-, T61A-, K192A- and NE232–233AA-expressing cells, respectively (Fig. 3E). Combined with the pull-down data described above, these results show that single alanine substitutions within the DH-domain of Cb II reduce, and the NE232–233AA double mutation, efficiently abrogates induction of filopodia formation, i.e. Cdc42-mediated signalling.

Cdc42 activation is not required for the formation of submembranous gephyrin microclusters in 3T3 cells

We have shown that in HEK293 cells recombinant gephyrin accumulates in large intracellular aggregates (Kirsch & Betz, 1995). Upon coexpression of Cb II but not Cb I, small gephyrin microclusters are formed that colocalize with Cb II close to the plasma membrane (Kins *et al.*, 2000). To unravel whether this Cb II-dependent redistribution of gephyrin requires catalytic GEF activity, we analysed the subcellular distribution of GFP–gephyrin when either the DH-domain of Cb II or its downstream target, Cdc42, were inactivated in NIH-3T3 fibroblasts. As previously observed with HEK293 cells, recombinant GFP–gephyrin formed large intracellular aggregates in transfected 3T3 fibroblasts (Fig. 4A), and coexpression of Cb II resulted in approximately 50% of the cotransfected cells in the formation of GFP–gephyrin microclusters, which were partially localized at the cell periphery (Fig. 4B and I). In agreement with a previous report (Harvey *et al.*, 2004), deletion of the DH-domain blocked the ability of Cb II to produce GFP–gephyrin microclusters (data not shown) and also abolished its ability to form filopodia (supporting Fig. S3D). In contrast, coexpression of the partially inactive T61A or K192A Cb II mutants or the completely inactive NE232–233AA mutant produced the same redistribution of gephyrin into microclusters as seen in WT Cb II-coexpressing cells (Fig. 4B–E). Furthermore, active Cdc42 appeared to be dispensable for formation of gephyrin microclusters, as triple transfection of WT Cb II, gephyrin and either a Cdc42 dominant-negative mutant (Cdc42-T17N; Fig. 4F) or the Cdc42-binding domain of WASP (Fig. 4G) resulted in the efficient formation of GFP–gephyrin microclusters, even though filopodia formation was completely blocked by the latter construct (supporting Fig. S3E). The proportion of transfected cells showing GFP–gephyrin either (i) diffusely distributed, (ii) accumulated within intracellular aggregates (diameter > 3 μm; $n < 5$ per cell) or (iii) redistributed into peripheral microclusters (diameter < 1 μm; $n > 50$ per cell) is shown in Fig. 4I. These results show that Cdc42

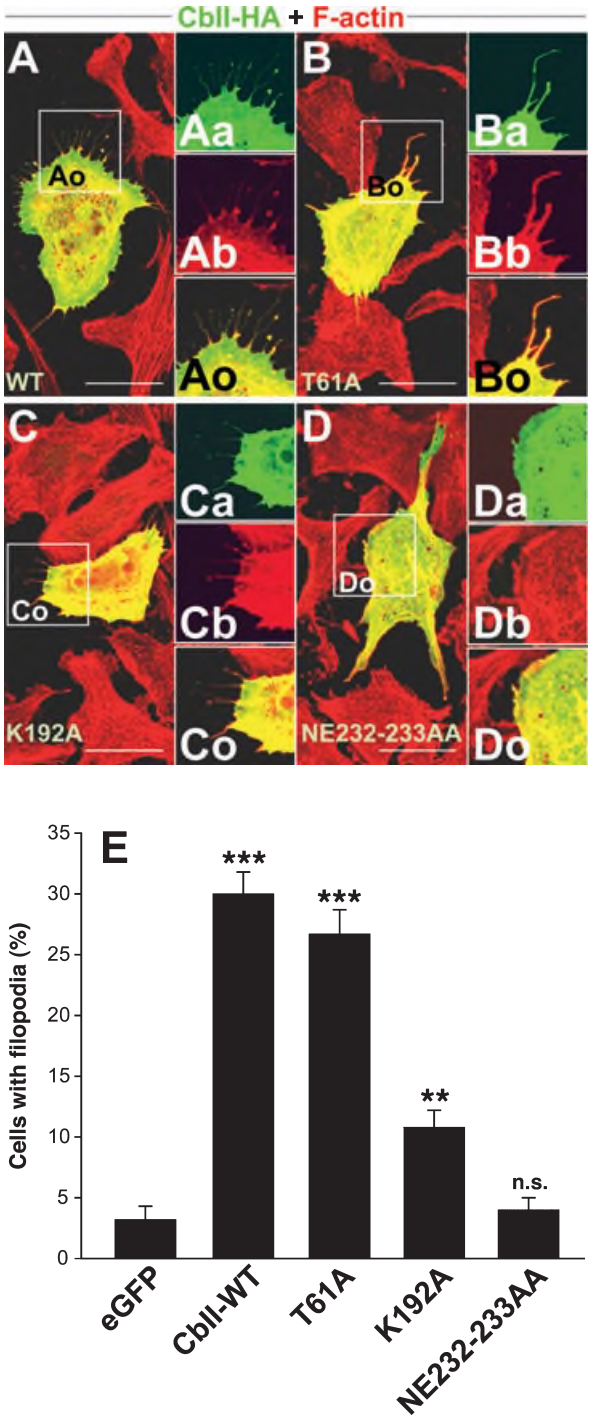

FIG. 3. Effect of Cb II DH-domain mutations on filopodia formation. (A–D) NIH-3T3 cells expressing (A) HA-tagged Cb II WT or the (B) T61A, (C) K192A or (D) NE232–233AA mutants. Cb II proteins were visualized with anti-HA immunostaining (green). Actin filaments were visualized with fluorescently labelled phalloidin (red). Single channels and overlays of the boxed areas in A–D are shown at higher magnification. Here, individual filopodia in Ao–Co are clearly discernible. Note the absence of filopodia in NE232–233AA transfected cells (D, Do). Scale bar = 16 μm. (E) Quantification of the percentage of transfected cells showing filopodia. eGFP, HA-tagged Cb II WT or the DH mutants were expressed in NIH-3T3 cells as described under Materials and methods, and 100 cells per transfection were examined for filopodia. Results are mean values (± SEM) obtained from three independent transfection experiments each (**$P < 0.01$; ***$P < 0.001$; ns: not significant; unpaired, two-tailed Student's t-test; $n = 3$).

activation is not required for the Cb II-induced redistribution of gephyrin into microclusters in 3T3 cells.

Cdc42 is not required for synaptic clustering of gephyrin and γ2-subunit-containing GABA$_A$Rs in the mammalian forebrain

To corroborate further that Cdc42 activation is not required for the clustering of gephyrin and gephyrin-dependent GABA$_A$Rs at inhibitory synapses, we performed gephyrin and GABA$_A$R-γ2 subunit stainings on brain sections derived from adult (postnatal day 90) Emx1$^{Cre/Cdc42\Delta ex2fl/fl}$ mice (Cappello *et al.*, 2006). In these mice, exon 2 of the Cdc42 gene is flanked by loxP sites (Wu *et al.*, 2006) and its deletion, directed by the empty spiracles homolog 1 (Emx1)::Cre gene (Iwasato *et al.*, 2000), has been shown to cause effective inactivation of Cdc42 in the cerebral cortex and hippocampus (Cappello *et al.*, 2006). Recombination in the Emx1::Cre mouse line (Iwasato *et al.*, 2000) starts at E9.5, leading to the loss of Cdc42 protein at E10/11 (Cappello *et al.*, 2006). Given the specific expression of Emx1 in cortical progenitors, recombination mediated by Cre driven by Emx1 affects exclusively glutamatergic neurons and glia in the cerebral cortex (Gorski *et al.*, 2002), as GABAergic neurons are derived from a different region of origin (Wonders & Anderson, 2005). Notably, 75% of the Emx1$^{Cre/Cdc42\Delta ex2fl/fl}$ mice born survive to adulthood; in these, only the lateral and piriform cortex show a normal layered organization, whereas most of the mutant cortex is severely disorganized. The hippocampal structures are no longer discernible, but have been found to persist as demonstrated by Math2 staining (Cappello *et al.*, 2006).

Here, the histological analysis of cresyl-violet-stained sections prepared from adult Emx1$^{Cre(-)/Cdc42\Delta ex2fl/+}$ controls (Ctrl) and Emx1$^{Cre/Cdc42\Delta ex2fl/fl}$ brains confirmed the severe disorganization of the hippocampus in the mutant animals (Fig. 5A and B). For the analysis of gephyrin and GABA$_A$R-γ2 subunit clusters, we focused on a region equivalent to the CA1 region of the stratum radiatum (SR) of the Ctrl brains (indicated by arrows in Fig. 5C and D). This region has been shown to exhibit a > 80% reduction in gephyrin and GABA$_A$R γ2-subunit cluster densities in Cb-deficient (Cb KO) mice (Papadopoulos *et al.*, 2007, 2008) and was identified here by visualization of the dense DAPI-stained nuclei in the stratum pyramidale (SP; Fig. 5E and F). Both in Ctrl and in Emx1$^{Cre/Cdc42\Delta ex2fl/fl}$ sections, punctate gephyrin immunoreactivity was found throughout the region adjacent to the SP, which was considered to be equivalent to the SR of the Ctrl hippocampi (Fig. 5G and H). Furthermore, in all forebrain regions of the Emx1$^{Cre/Cdc42\Delta ex2fl/fl}$ sections analysed, gephyrin immunoreactivity was concentrated in clusters that were similar to those of Ctrl sections, and large intracellular aggregates of gephyrin as observed in the SP of Cb KO mice (Papadopoulos *et al.*, 2007, 2008) were not detected (data not shown). Also, the gephyrin clusters exhibited a high level of colocalization with clusters immunopositive for the γ2-subunit of GABA$_A$Rs in both genotypes (Fig. 5I and J), consistent with an unaffected recruitment of these receptors to gephyrin-positive sites in the forebrain of Emx1$^{Cre/Cdc42\Delta ex2fl/fl}$ mice. Quantification of the numbers of gephyrin- and γ2-positive clusters per 500 μm^2 SR area revealed values of 178.2 ± 6.6 vs. 181.0 ± 5.3 for gephyrin, and of 164.0 ± 4.9 vs. 171.2 ± 3.0 for the γ2-subunit, in Ctrl and Emx1$^{Cre/Cdc42\Delta ex2fl/fl}$ samples, respectively (Fig. 5K). These results indicate that the clustering of gephyrin- and γ2-subunit-containing GABA$_A$Rs within the dendritic compartment of pyramidal neurons derived from Emx1$^{Cre/Cdc42\Delta ex2fl/fl}$ mice is similar to that obtained from Ctrl mice, further supporting our conclusion that activation of Cdc42 by Cb is not required for inhibitory synapse formation.

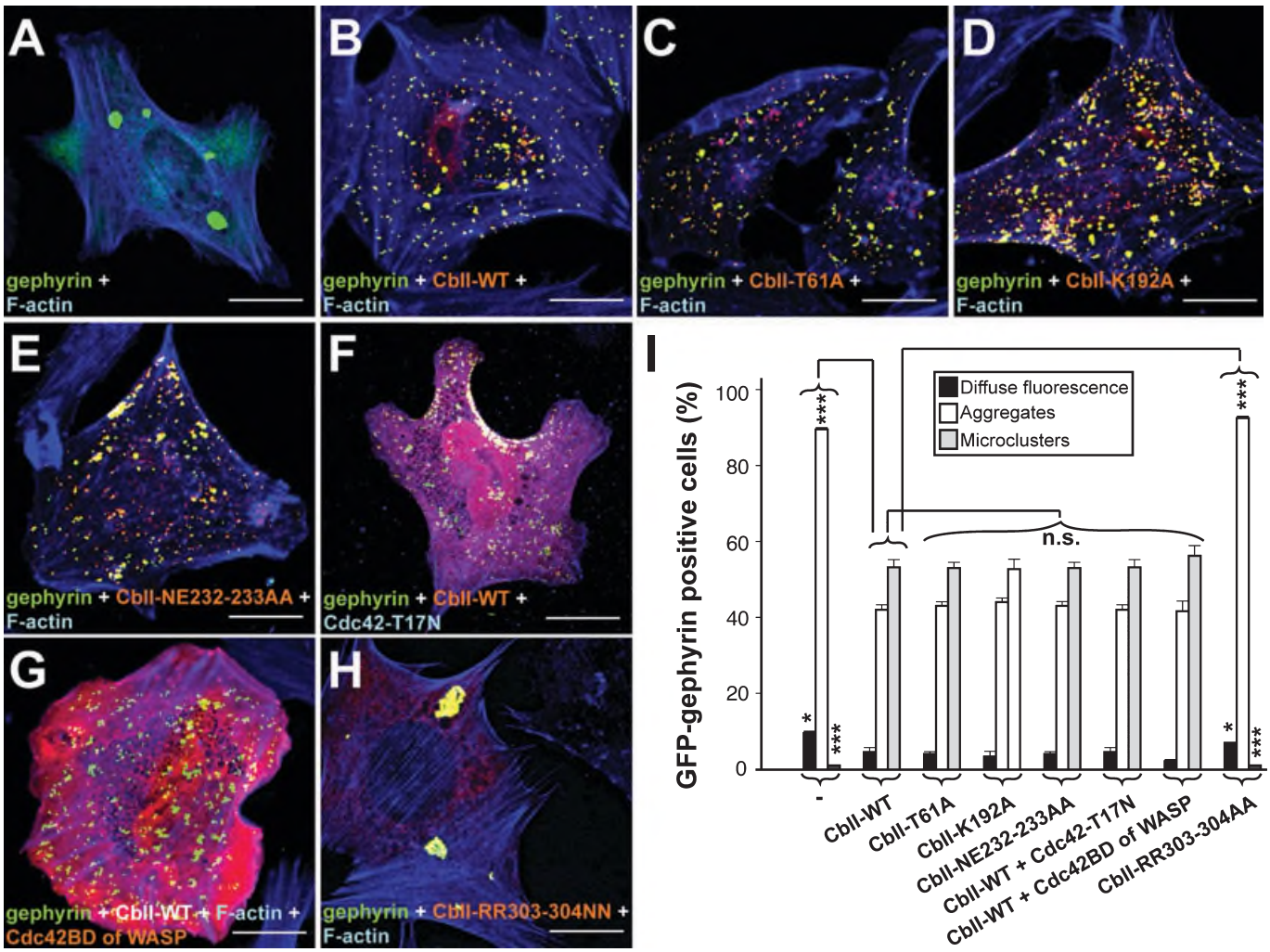

FIG. 4. Cdc42-independent formation of gephyrin microclusters in 3T3 cells. (A–H) NIH-3T3 cells expressing either (A) GFP–gephyrin alone, or together with (B) HA-tagged Cb II WT, (C) T31A, (D) K192A, (E) NE232–233AA, (F) Cb II WT + Myc-tagged Cdc42 T17N, (G) Cb II WT + Myc-tagged Cdc42BD of WASP, or (H) the PH-domain double mutant RR303–304NN. Actin filaments were visualized with fluorescently labelled phalloidin (blue). Upon single expression, GFP–gephyrin was concentrated in large intracellular aggregates (A). All the DH-domain mutations analysed produced a redistribution of gephyrin into peripheral microclusters as seen with Cb II WT (B–E). Similarly, the T17N dominant-negative mutant of Cdc42 (F) as well as the Cdc42BD of WASP (G) did not block Cb II-induced gephyrin microcluster formation. In contrast, an absence of microclusters and an accumulation of gephyrin within large intracellular aggregates was found in cells expressing the PH-domain mutant RR303–304NN (H). Scale bar = 16 μm. (I) Quantification of the percentage of GFP–gephyrin cotransfected cells showing gephyrin either (i) diffusely distributed in the cell body (black bars), (ii) concentrated in large intracellular aggregates (white bars; diameter > 3 μm; $n < 5$ per cell) or (iii) localized within microclusters (grey bars; diameter < 1 μm; $n > 50$ per cell). Results are mean values (± SEM) obtained from three independent transfection experiments each (*$P < 0.05$; ***$P < 0.001$; ns: not significant; unpaired, two-tailed Student's t-test; $n = 3$).

PH-Domain-driven targeting of Cb II is required for the formation of gephyrin clusters at inhibitory synapses

A previous study (Harvey *et al.*, 2004) has suggested that the PH-domain of Cb II is required for the synaptic targeting of gephyrin, as deletion of this domain resulted in both the accumulation of cytoplasmic Cb II-gephyrin co-aggregates in cotransfected HEK293 cells and a loss of dendritic gephyrin clusters upon expression of the deletion mutant in dissociated rat cortical neurons. In addition, deletion of the PH-domain of Cb has been found to abolish PI3P binding without affecting interactions with gephyrin via the Cb RhoGEF domain (Kalscheuer *et al.*, 2009). However, from these results it is not clear whether the deletion of the entire Cb PH-domain disrupts only phoshoinositide binding or additional interactions with other proteins, which might contribute to the proper localization of gephyrin at inhibitory postsynaptic sites. To examine further whether lipid interactions of the PH-domain are required for synaptic gephyrin clustering, we generated a Cb II mutant in which the arginine residues R303 and R304 were both replaced by asparagines. These residues reside within the $\beta3$–$\beta4$ loop of the PH-domain of Cb, and their positively charged side chains are surface-exposed (Fig. 1B). The positively charged surface of the $\beta1$–$\beta2$ and $\beta3$–$\beta4$ loops of several PH-domains has been previously shown to be involved in membrane lipid anchoring (Hyvonen *et al.*, 1995; Yu *et al.*, 2004; DiNitto & Lambright, 2006). Using immobilized PI3P and purified GST-tagged Cb II and GST-Cb II-RR303–304NN in a lipid overlay assay as described previously (Kalscheuer *et al.*, 2009; supporting Appendix S1), we confirmed that the RR303–304 residues are essential for CbII binding to this phosphoinositide (supporting Fig. S4; see also Soykan *et al.*, 2009). In contrast to what was seen with the RhoGEF mutants described above, coexpression of the RR303–304NN mutant with gephyrin in NIH 3T3 cells resulted in the formation of intracellular aggregates, in which both gephyrin and the mutant protein were perfectly colocalized (Fig. 4H). The

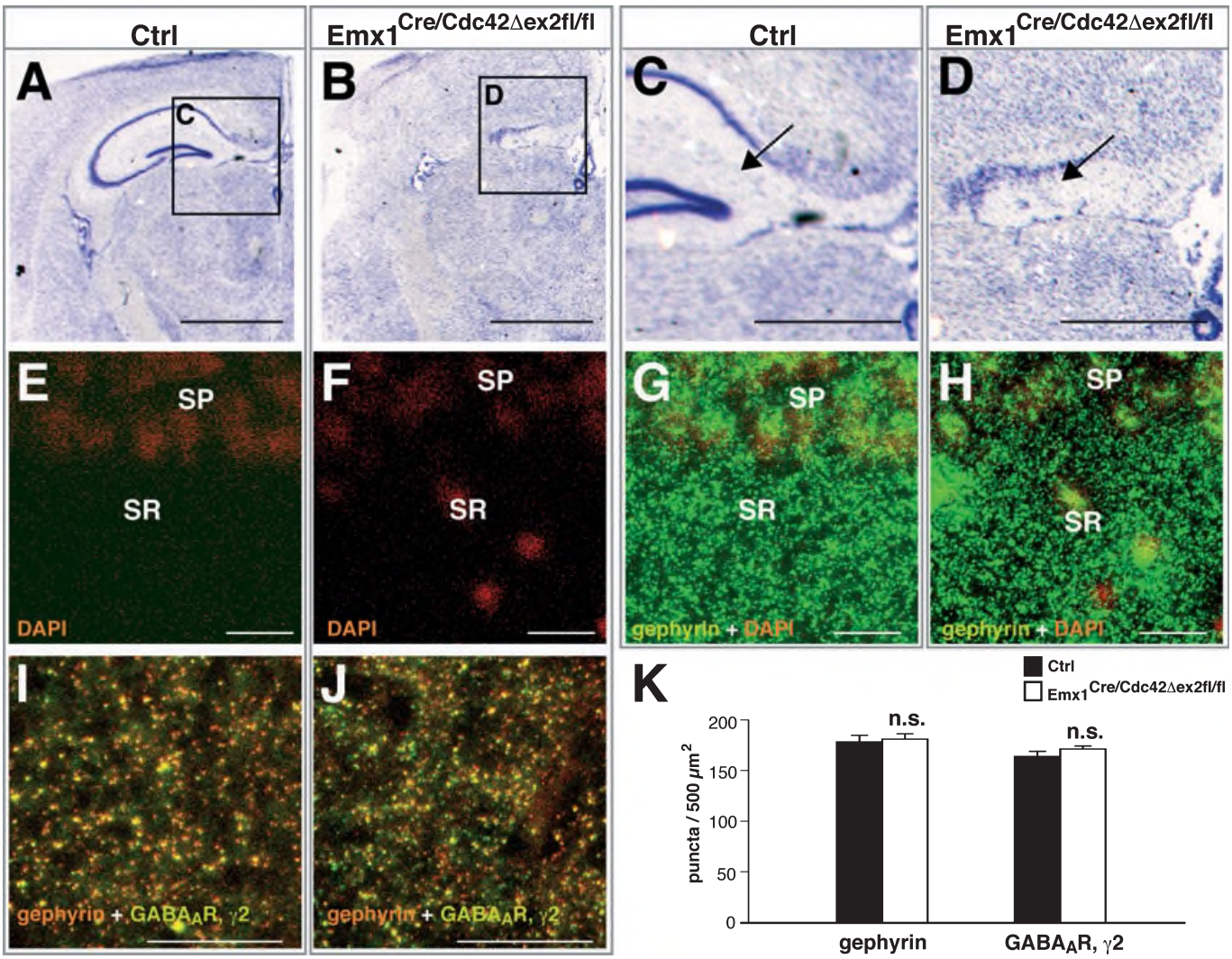

FIG. 5. Gephyrin and $GABA_AR$ γ2-subunit clusters in the hippocampus of $Emx1^{Cre/Cdc42\Delta ex2fl/fl}$ mice. (A and B) Cresyl-violet-stained coronal sections from brains of $Emx1^{Cre/Cdc42\Delta ex2fl/fl}$ mice (B) and Cre-negative Ctrl ($Emx1^{Cre(-)/Cdc42\Delta ex2fl/+}$) littermates (A). (C and D) Boxed areas in A and B shown at higher magnification. Arrows indicate the SR CA1 region. Note loss of cellular layers in the Cdc42-deficient hippocampus. (E and F) DAPI-stained nuclei for visualization of the stratum pyramidale (SP) and the stratum radiation (SR) CA1 region in hippocampal sections from Ctrl (E) and mutant (F) brains. (G and H) The same sections were costained with the gephyrin-specific 7a monoclonal antibody (green) and processed for immunofluorescence microscopy. (I and J) Brain sections through the SR CA1 regions of Ctrl (I) and mutant (J) mice were stained with monoclonal antibody 7a (red) and an antibody specific for the γ2-subunit of $GABA_ARs$ (green). Scale bars = 1.6 mm (A, B), 0.8 mm (C, D), 16 μm (E–J). (K) Quantification of gephyrin and $GABA_AR$ γ2-subunit immunoreactive cluster densities per 500 μm^2 area in the SR CA1 of Ctrl and of $Emx1^{Cre/Cdc42\Delta ex2fl/fl}$ mice. Each bar corresponds to mean values (± SEM) obtained with sections from three individual brains (ns: not significant; unpaired, two-tailed Student's *t*-test; $n = 3$).

percentage of cells showing cytoplasmic aggregates was similar to that observed upon single GFP–gephyrin expression (Fig. 4I).

To assess whether phosphoinositide binding activity of Cb contributes to gephyrin clustering at inhibitory synapses, we cotransfected GFP–gephyrin with WT Cb II, Cb II NE232–233AA, or Cb II RR303–304NN into cultured hippocampal neurons. Among the RhoGEF-deficient mutants of Cb II tested, the NE232–233AA mutant was selected for these experiments, as it did not display any exchange activity toward Cdc42 (see Figs 2B and 3E). Figure 6A shows that dendrites of neurons transfected with WT Cb II carried a high density of GFP–gephyrin clusters which colocalized with recombinant Cb II. Up to 56% of these clusters were synaptic, as indicated by their apposition to VIAAT immunoreactivity (Fig. 6Ao). Similarly, the NE232–233AA mutant of Cb II had no effect on GFP–gephyrin clustering (Fig. 6B), and no obvious difference could be seen in dendritic gephyrin puncta between WT and NE232–233AA transfected neurons (compare Fig. 6A–Ao with Fig. 6B–Bo). In contrast, neurons cotransfected with Cb II RR303–304NN contained large intracellular GFP–gephyrin aggregates that colocalized with this PH-domain-specific mutant (Fig. 6C). Similar intracellular aggregates of gephyrin were also observed in neurons expressing WT Cb II (data not shown) and Cb II NE232–233AA (Fig. 6B) and might be due to the overexpression of the recombinant proteins. However, in the WT Cb II and NE232–233AA transfected cells, these aggregates were always accompanied by a high density of smaller gephyrin clusters at inhibitory postsynaptic sites. In contrast, GFP–gephyrin clusters were either lacking or strikingly reduced in the dendrites of neurons cotransfected with the Cb II RR303–304NN mutant (Fig. 6C-Co). As single expression of GFP–gephyrin in neurons generates high densities of GFP-positive clusters apposed to VIAAT at inhibitory synapses (Saiyed *et al.*, 2007; and data not shown), the RR303–304NN mutant apparently competes with endogenous Cb for binding

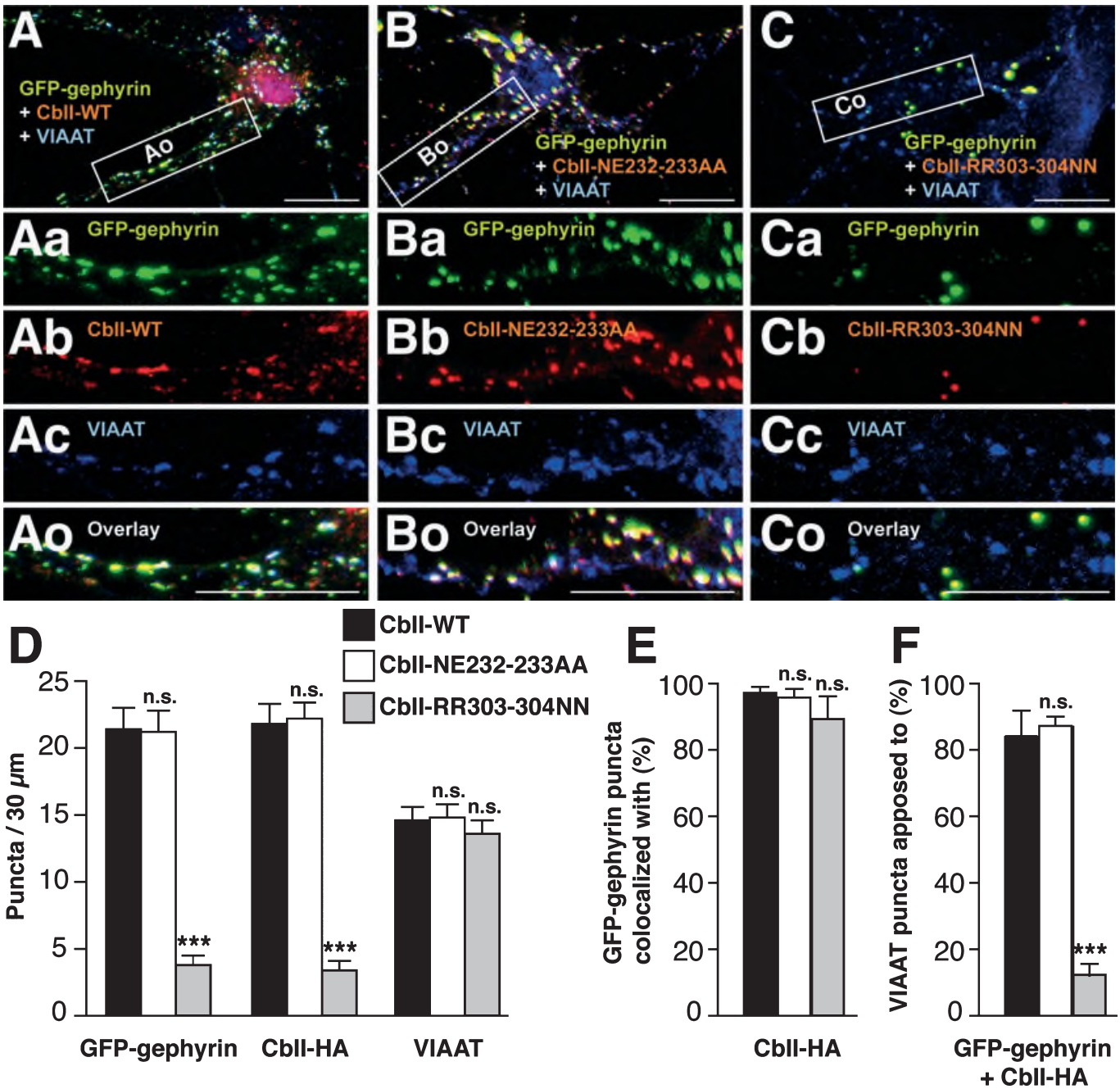

FIG. 6. The Cb II RR303–304NN but not the NE232–233AA mutation impairs synaptic clustering of GFP–gephyrin in cultured hippocampal neurons. (A–C) cDNA encoding GFP–gephyrin was transfected together with HA-tagged Cb II WT (A) or the NE232–233AA (B), or the RR303–304NN (C) mutants into cultured rat hippocampal neurons at day 10 *in vitro* (DIV10). At DIV 23, neurons were fixed and stained with anti-HA (red) and anti-VIAAT (blue) antibodies. (Aa–o, Ba–o, Ca–o) Single channels and overlays of the boxed areas in A–C shown at higher magnification. Note the strong reduction of synaptically localized (as monitored by VIAAT immunolabelling; Ac–Cc) GFP–gephyrin in neurons cotransfected with the Cb II RR303–304NN mutant (Cb, Co) as compared with neurons cotransfected with Cb II WT (Ab, Ao), or with NE232–233AA (Bb, Bo), respectively. Scale bars = 16 μm. (D–F) Quantification of GFP–gephyrin, Cb II and VIAAT immunoreactivities (D) and colocalization of GFP-gephyrin with CbII-HA proteins (E), and of VIAAT with GFP-gephyrin and CbII-HA (FA), respectively. Puncta per 30 μm dendritic length were counted and compared for colocalization. Note the strong reduction of GFP–gephyrin and RR303–304NN puncta in the dendrites of neurons cotransfected with this mutant as compared with neurons transfected with Cb II WT or the NE232–233AA mutant. Each bar corresponds to counts performed on randomly selected dendrites of five individuall cells per transfection experiment. Data represent means ± SEM obtained from three independent transfection experiments each (***$P < 0.001$; ns: not significant; Student's t test; $n = 3$).

to gephyrin. The RR303–304NN cotransfected neurons did not significantly differ from neurons expressing WT Cb II or the NE232–233AA mutant in VIAAT punctate immunoreactivity (Fig. 6C and D), indicating that the loss of gephyrin and Cb II clusters does not reflect reduced inhibitory innervation. Quantification of the number of GFP–gephyrin clusters per 30 μm^2 dendritic length revealed values of 21.4 ± 1.6, 21.2 ± 1.6 and 3.8 ± 0.7 for WT Cb II, NE232–233AA and RR303–304NN cotransfected neurons, respectively (Fig. 6D). Thus, the RR303–304NN, but not the NE232–233AA, substitution impairs Cb II-mediated gephyrin clustering. Notably, the percentage of

the remaining gephyrin clusters colocalizing with Cb II was not altered with either of the mutant proteins (Fig. 6E). However, the percentage of VIAAT-positive puncta apposed to GFP–gephyrin-Cb II double positive clusters was strikingly reduced for RR303–304NN as compared with WT Cb II and NE232–233AA cotransfected cells (Fig. 6F). Taken together, these results indicate that specific interactions of the PH-domain of Cb with membrane phospholipids such as PI3P are required for the targeting of gephyrin to inhibitory synapses, but not the catalytic activity of Cb towards Cdc42.

Discussion

The reactions underlying the Cb-mediated formation and stabilization of gephyrin scaffolds at inhibitory postsynapses remain to be fully characterized. Given the recent progress in our understanding of Cb I activation by NL2 at inhibitory postsynaptic sites (Poulopoulos *et al.*, 2009), a central question concerns the signalling mechanisms by which activated Cb induces gephyrin recruitment, i.e. its potential role as a synaptically active GEF. Here, we focused on the constitutively active splice variant Cb II, as this variant is more effective in catalysing nucleotide exchange at Cdc42. The specific interaction between Cb II and Cdc42 suggested that Cdc42 activation by Cb II is important for gephyrin clustering (Reid *et al.*, 1999; Xiang *et al.*, 2006). However, our analysis of Cb II DH-domain mutants and Cdc42 conditional knockout mice demonstrates that Cdc42 activation is not involved in inhibitory synapse formation. The data presented here clearly show that Cb has at least two distinct biological functions, the DH-domain-dependent activation of Cdc42 required for the induction of filopodia and the Cdc42-independent, PH-domain-mediated formation of gephyrin scaffolds at inhibitory postsynaptic sites.

The NE232–233AA mutation eliminates Cdc42-induced filopodia formation in 3T3 cells

Among the DH-domain mutants characterized here, the NE232–233AA mutant did not catalyse any GDP/GTP exchange on Cdc42, as revealed by GST-PAK1-PBD pulldown *in vitro* (Fig. 2). This result is in agreement with previous mutagenesis studies on highly conserved residues of several Dbl family GEFs corresponding to N232 and E233 in Cb (Zhu *et al.*, 2000; Debreceni *et al.*, 2004; Schiller *et al.*, 2005) and underlines the critical role of these residues in GEF catalytic activity towards Cdc42. Also, upon ectopic expression in NIH-3T3 cells, the NE232–233AA mutant failed to induce filopodia formation as found with WT Cb II (Fig. 3). This is consistent with a Rho GTPase-sequestering role of this mutant and is reminiscent of the cellular effects seen with the Cb IIΔDH mutant (Harvey *et al.*, 2004) or upon coexpression of the Cdc42BD of WASP with WT Cb II (supporting Fig. S3). In contrast, the T61A and K192A mutants displayed partial GEF activity towards Cdc42 and caused significant actin cytoskeleton rearrangements upon overexpression in NIH-3T3 cells (Figs 2 and 3). A similar result has been reported for Trio substituted at T1244, i.e. the residue corresponding to T61 in Cb II (Debreceni *et al.*, 2004). In conclusion, we have identified a conserved pair of amino acid residues of the Cb II–Cdc42 complex that is essential for both Cb's GEF activity towards Cdc42 and filopodia formation.

Gephyrin scaffold formation is independent of Cdc42 activation

Deletion of the DH-domain of Cb impairs gephyrin targeting to inhibitory postsynaptic sites (Harvey *et al.*, 2004). However, whether the catalytic GEF activity of Cb and Cdc42 activation is essential for inhibitory synapse formation had not been examined. Here, we demonstrate that DH-domain substitutions which fully eliminate Cdc42 activation, e.g. the NE232–233AA double mutation, do not affect Cb-dependent gephyrin recruitment into microclusters upon coexpression in NIH-3T3 cells. This suggests that the Rho-GTPase Cdc42 is not required for submembrane targeting of gephyrin. Consistent with this view, overexpression of a dominant-negative mutant of Cdc42 (T17N), or of the Cdc42 binding domain of WASP, together with Cb II and gephyrin had no effect on gephyrin's subcellular distribution as compared with Cb II and gephyrin cotransfected cells (Fig. 4). To examine further the importance of Cdc42 in regulating gephyrin scaffold formation, we used a previously described Cdc42 conditional knockout mouse line ($Emx1^{Cre/Cdc42\Delta ex2fl/fl}$), in which the Cdc42 gene is inactivated in the forebrain (Cappello *et al.*, 2006). Ablation of Cdc42 led to unaltered gephyrin and $GABA_AR$ γ2-subunit cluster densities in the SR CA1 area of the hippocampus, as compared with WT. As this hippocampal region shows a > 80% loss of gephyrin and $GABA_AR$ γ2-subunit clusters in mice lacking Cb (Papadopoulos *et al.*, 2007), Cb cannot serve as a signal transducer for inhibitory synapse formation by activating Cdc42, as proposed previously (Kneussel & Betz, 2000). However, recruitment of Cb to inhibitory postsynaptic sites through a mechanism involving NL2–gephyrin and NL2–Cb interactions is important for the inhibitory synapse-specific localization of the gephyrin scaffold (Poulopoulos *et al.*, 2009). Similarly, at excitatory synapses, NL3 recruits Epac2 (exchange protein directly activated by cAMP; also known as cAMP-GEFII and RapGEF4), a GEF for Rap, to the plasma membrane and enhances its Rap-GEF activity, thereby promoting increased spine dynamics (Woolfrey *et al.*, 2009).

In conclusion, inhibitory synapse formation cannot be attributed to Cdc42 activation. However, we cannot rule out that other, as yet unidentified Rho-like GTPases are activated by Cb at synaptic sites. Dbl-family proteins display varied selectivities, and analyses have been mainly carried out for Cdc42, Rac1 and RhoA (Reid *et al.*, 1999; Schmidt & Hall, 2002). Non-conserved residues that reside within the interface between DH-domains and GTPases are likely candidates for determining specific coupling. This interface differs significantly between GTPases (Worthylake *et al.*, 2000). A possible scenario could be that the DH-domain of Cb can discriminate among different G-proteins, thus regulating the spatio-temporal activation of more than one Rho-GTPase in response to dinstict stimuli. We expect that future experiments will identify additional Cb cognate Rho-GTPases and thus provide information on how this GEF contributes to the development of inhibitory synapses.

PH-Domain-driven targeting of Cb is required for synaptic gephyrin clustering

PH-Domains are best known for their ability to bind phosphoinositides and to be targeted to cellular membranes (Hyvonen *et al.*, 1995). Alternatively, PH-domains that do not bind phosphoinositides may be membrane targeted by binding to other ligands, and some of them may not be associated with membranes at all (Yu *et al.*, 2004). In the case of Cb, previous studies have shown that the PH-domain interacts specifically with PI3P, and that deletion of the entire domain causes a loss of synaptic gephyrin and $GABA_AR$ clusters, presumably due to a dominant-negative mechanism (Harvey *et al.*, 2004; Kalscheuer *et al.*, 2009). This result is consistent with phospholipid binding of Cb's PH-domain being important for

postsynaptic membrane targeting. However, in the GEF Dbs (the 'big sister' of Dbl) PH-domain residues have been found to be critical for side chain electron polarization within the DH-domain and in facilitating efficient guanine nucleotide exchange on its cognate GTP-binding protein (Rossman *et al.*, 2002). Thus, deletion of the entire PH-domain might affect both phospholipid binding and Rho-GTPase activation. In an attempt to identify specific side chains within the PH-domain that are involved in lipid interactions and to disclose whether PI3P binding is essential for gephyrin clustering, we replaced the two adjacent arginine residues (R303 and R304) by asparagines. These basic residues have been recently shown to be involved in PI3P binding to Cb (Soykan *et al.*, 2009) and to reside within the $\beta3$–$\beta4$ loop of the PH-domain, with their positively charged side chains exposed to the surface (Fig. 1B). The positively charged surface of the $\beta x/\beta x + 1$ loop of several PH-domains is known to be essential for phosphoinositide binding (Yu *et al.*, 2004). In both NIH-3T3 cells and cultured hippocampal neurons, coexpression of the RR303–304NN mutant together with GFP–gephyrin led to the formation of large intracellular GFP–gephyrin aggregates and to a strong reduction of synaptically localized GFP–gephyrin clusters colocalizing with the epitope-tagged Cb II protein (Figs 4 and 6). Thus, the inability of Cb II to bind efficiently to PI3P has important consequences for its recruitment to cellular membranes together with gephyrin, a process that is essential for proper gephyrin scaffold formation at developing postsynaptic sites.

Further work will be required to unravel the molecular mechanisms underlying the PH-domain-assisted targeting of Cb and gephyrin to synapses. GEF mutants that eliminate the binding of phosphoinositides to the PH-domain do not activate their cognate GTPases *in vivo* (Baumeister *et al.*, 2003; Rossman *et al.*, 2003; Skowronek *et al.*, 2004). This suggests that conformational changes in these GEFs are required to relieve a steric block of the active site by the PH-domain. Future experiments aimed at deciphering the mechanism of Cb activation, identifying interactions of Cb with other Rho GTPases, and elucidating conformational changes induced upon phosphoinositide and NL2 binding should help to unravel how the formation of inhibitory postsynapses is regulated.

Supporting Information

Additional supporting information may be found in the online version of this article:

Fig. S1. GST-PAK1 PBD affinity precipitation of GTP-bound Cdc42.

Fig. S2. The effects of constitutively active forms of Cdc42, Rac1 and RhoA on actin cytoskeleton reorganization.

Fig. S3. Both Cb I and Cb II induce the formation of filopodia in 3T3 cells.

Fig. S4. Residues R303 and R304 are required for proper binding of CbII to PI3P.

Appendix S1. Supplementary materials and methods.

Please note: As a service to our authors and readers, this journal provides supporting information supplied by the authors. Such materials are peer-reviewed and may be re-organized for online delivery, but are not copy-edited or typeset by Wiley-Blackwell. Technical support issues arising from supporting information (other than missing files) should be addressed to the authors.

Acknowledgements

We thank Dr Jean-Marc Fritschy for providing the antibody against the $GABA_AR$ $\gamma2$-subunit, Dr Alan Hall for providing the plasmid of the pRK5Myc-Cdc42 binding domain of WASP, and Ina Bartnik and Belquis Nassim-Assir for excellent technical assistance. This work was supported by the Max-Planck-Gesellschaft, Deutsche Forschungsgemeinschaft (SFB-628/P15 and Cluster of Excellence EXC 115 'Macromolecular Complexes') and Fonds der Chemischen Industrie.

Abbreviations

Cb, collybistin; DH, Dbl-homology; $GABA_AR$, γ-aminobutyric acid receptor; GEF, guanine nucleotide exchange factor; GlyR, glycine receptor; GST, glutathione-S-transferase; HA, haemagglutinin; HEK, human embryonic kidney; PBD, p21-binding domain; PH, pleckstrin homology; PI3P, phosphatidylinositol-3-phosphate; SH3, Src homology 3; SP, stratum pyramidale; SR, stratum radiatum; VIAAT, vesicular inhibitory amino acid transporter; WASP, Wiskott-Aldrich syndrome protein; WT, wild-type.

References

Aghazadeh, B., Zhu, K., Kubiseski, T.J., Liu, G.A., Pawson, T., Zheng, Y. & Rosen, M.K. (1998) Structure and mutagenesis of the Dbl homology domain. *Nat. Struct. Biol.*, **5**, 1098–1107.

Armsen, W., Himmel, B., Betz, H. & Eulenburg, V. (2007) The C-terminal PDZ-ligand motif of the neuronal glycine transporter GlyT2 is required for efficient synaptic localization. *Mol. Cell. Neurosci.*, **36**, 369–380.

Aspenstrom, P., Lindberg, U. & Hall, A. (1996) Two GTPases, Cdc42 and Rac, bind directly to a protein implicated in the immunodeficiency disorder Wiskott-Aldrich syndrome. *Curr. Biol.*, **6**, 70–75.

Baumeister, M.A., Martinu, L., Rossman, K.L., Sondek, J., Lemmon, M.A. & Chou, M.M. (2003) Loss of phosphatidylinositol 3-phosphate binding by the C-terminal Tiam-1 pleckstrin homology domain prevents in vivo Rac1 activation without affecting membrane targeting. *J. Biol. Chem.*, **278**, 11457–11464.

Bausen, M., Fuhrmann, J.C., Betz, H. & O'Sullivan, G.A. (2006) The state of the actin cytoskeleton determines its association with gephyrin: role of ena/VASP family members. *Mol. Cell. Neurosci.*, **31**, 376–386.

Cappello, S., Attardo, A., Wu, X., Iwasato, T., Itohara, S., Wilsch-Brauninger, M., Eilken, H.M., Rieger, M.A., Schroeder, T.T., Huttner, W.B., Brakebusch, C. & Gotz, M. (2006) The Rho-GTPase cdc42 regulates neural progenitor fate at the apical surface. *Nat. Neurosci.*, **9**, 1099–1107.

Chih, B., Engelman, H. & Scheiffele, P. (2005) Control of excitatory and inhibitory synapse formation by neuroligins. *Science*, **307**, 1324–1328.

Craig, A.M. & Kang, Y. (2007) Neurexin-neuroligin signaling in synapse development. *Curr. Opin. Neurobiol.*, **17**, 43–52.

Debreceni, B., Gao, Y., Guo, F., Zhu, K., Jia, B. & Zheng, Y. (2004) Mechanisms of guanine nucleotide exchange and Rac-mediated signaling revealed by a dominant negative trio mutant. *J. Biol. Chem.*, **279**, 3777–3786.

DiNitto, J.P. & Lambright, D.G. (2006) Membrane and juxtamembrane targeting by PH and PTB domains. *Biochim. Biophys. Acta*, **1761**, 850–867.

Fritschy, J.M., Harvey, R.J. & Schwarz, G. (2008) Gephyrin: where do we stand, where do we go? *Trends Neurosci.*, **31**, 257–264.

Fuhrmann, J.C., Kins, S., Rostaing, P., El Far, O., Kirsch, J., Sheng, M., Triller, A., Betz, H. & Kneussel, M. (2002) Gephyrin interacts with Dynein light chains 1 and 2, components of motor protein complexes. *J. Neurosci.*, **22**, 5393–5402.

Gorski, J.A., Talley, T., Qiu, M., Puelles, L., Rubenstein, J.L. & Jones, K.R. (2002) Cortical excitatory neurons and glia, but not GABAergic neurons, are produced in the Emx1-expressing lineage. *J. Neurosci.*, **22**, 6309–6314.

Hall, A. (1998) Rho GTPases and the actin cytoskeleton. *Science*, **279**, 509–514.

Hamann, M.J., Lubking, C.M., Luchini, D.N. & Billadeau, D.D. (2007) Asef2 functions as a Cdc42 exchange factor and is stimulated by the release of an autoinhibitory module from a concealed C-terminal activation element. *Mol. Cell. Biol.*, **27**, 1380–1393.

Harvey, K., Duguid, I.C., Alldred, M.J., Beatty, S.E., Ward, H., Keep, N.H., Lingenfelter, S.E., Pearce, B.R., Lundgren, J., Owen, M.J., Smart, T.G., Luscher, B., Rees, M.I. & Harvey, R.J. (2004) The GDP-GTP exchange factor collybistin: an essential determinant of neuronal gephyrin clustering. *J. Neurosci.*, **24**, 5816–5826.

Hyvonen, M., Macias, M.J., Nilges, M., Oschkinat, H., Saraste, M. & Wilmanns, M. (1995) Structure of the binding site for inositol phosphates in a PH domain. *EMBO J.*, **14**, 4676–4685.

Iwasato, T., Datwani, A., Wolf, A.M., Nishiyama, H., Taguchi, Y., Tonegawa, S., Knopfel, T., Erzurumlu, R.S. & Itohara, S. (2000) Cortex-restricted disruption of NMDAR1 impairs neuronal patterns in the barrel cortex. *Nature*, **406**, 726–731.

Jamain, S., Radyushkin, K., Hammerschmidt, K., Granon, S., Boretius, S., Varoqueaux, F., Ramanantsoa, N., Gallego, J., Ronnenberg, A., Winter, D., Frahm, J., Fischer, J., Bourgeron, T., Ehrenreich, H. & Brose, N. (2008) Reduced social interaction and ultrasonic communication in a mouse model of monogenic heritable autism. *Proc. Natl Acad. Sci. USA*, **105**, 1710–1715.

Jiang, Q., Gu, Z., Zhang, G. & Jing, G. (2000) Diphosphorylation and involvement of extracellular signal-regulated kinases (ERK1/2) in glutamate-induced apoptotic-like death in cultured rat cortical neurons. *Brain Res.*, **857**, 71–77.

Kalscheuer, V.M., Musante, L., Fang, C., Hoffmann, K., Fuchs, C., Carta, E., Deas, E., Venkateswarlu, K., Menzel, C., Ullmann, R., Tommerup, N., Dalpra, L., Tzschach, A., Selicorni, A., Luscher, B., Ropers, H.H., Harvey, K. & Harvey, R.J. (2009) A balanced chromosomal translocation disrupting ARHGEF9 is associated with epilepsy, anxiety, aggression, and mental retardation. *Hum. Mutat.*, **30**, 61–68.

Kins, S., Betz, H. & Kirsch, J. (2000) Collybistin, a newly identified brain-specific GEF, induces submembrane clustering of gephyrin. *Nat. Neurosci.*, **3**, 22–29.

Kirsch, J. & Betz, H. (1995) The postsynaptic localization of the glycine receptor-associated protein gephyrin is regulated by the cytoskeleton. *J. Neurosci.*, **15**, 4148–4156.

Kneussel, M. & Betz, H. (2000) Clustering of inhibitory neurotransmitter receptors at developing postsynaptic sites: the membrane activation model. *Trends Neurosci.*, **23**, 429–435.

Kolluri, R., Tolias, K.F., Carpenter, C.L., Rosen, F.S. & Kirchhausen, T. (1996) Direct interaction of the Wiskott-Aldrich syndrome protein with the GTPase Cdc42. *Proc. Natl Acad. Sci. USA*, **93**, 5615–5618.

Liu, X., Wang, H., Eberstadt, M., Schnuchel, A., Olejniczak, E.T., Meadows, R.P., Schkeryantz, J.M., Janowick, D.A., Harlan, J.E., Harris, E.A., Staunton, D.E. & Fesik, S.W. (1998) NMR structure and mutagenesis of the N-terminal Dbl homology domain of the nucleotide exchange factor Trio. *Cell*, **95**, 269–277.

Luo, L. (2000) Rho GTPases in neuronal morphogenesis. *Nat. Rev. Neurosci.*, **1**, 173–180.

Ma, X.M., Kiraly, D.D., Gaier, E.D., Wang, Y., Kim, E.J., Levine, E.S., Eipper, B.A. & Mains, R.E. (2008a) Kalirin-7 is required for synaptic structure and function. *J. Neurosci.*, **28**, 12368–12382.

Ma, X.M., Wang, Y., Ferraro, F., Mains, R.E. & Eipper, B.A. (2008b) Kalirin-7 is an essential component of both shaft and spine excitatory synapses in hippocampal interneurons. *J. Neurosci.*, **28**, 711–724.

Manser, E., Leung, T., Salihuddin, H., Zhao, Z.S. & Lim, L. (1994) A brain serine/threonine protein kinase activated by Cdc42 and Rac1. *Nature*, **367**, 40–46.

Mitin, N., Betts, L., Yohe, M.E., Der, C.J., Sondek, J. & Rossman, K.L. (2007) Release of autoinhibition of ASEF by APC leads to CDC42 activation and tumor suppression. *Nat. Struct. Mol. Biol.*, **14**, 814–823.

Nobes, C.D. & Hall, A. (1995) Rho, rac, and cdc42 GTPases regulate the assembly of multimolecular focal complexes associated with actin stress fibers, lamellipodia, and filopodia. *Cell*, **81**, 53–62.

Papadopoulos, T., Korte, M., Eulenburg, V., Kubota, H., Retiounskaia, M., Harvey, R.J., Harvey, K., O'Sullivan, G.A., Laube, B., Hulsmann, S., Geiger, J.R. & Betz, H. (2007) Impaired GABAergic transmission and altered hippocampal synaptic plasticity in collybistin-deficient mice. *EMBO J.*, **26**, 3888–3899.

Papadopoulos, T., Eulenburg, V., Reddy-Alla, S., Mansuy, I.M., Li, Y. & Betz, H. (2008) Collybistin is required for both the formation and maintenance of GABAergic postsynapses in the hippocampus. *Mol. Cell. Neurosci.*, **39**, 161–169.

Penzes, P., Johnson, R.C., Sattler, R., Zhang, X., Huganir, R.L., Kambampati, V., Mains, R.E. & Eipper, B.A. (2001) The neuronal Rho-GEF Kalirin-7 interacts with PDZ domain-containing proteins and regulates dendritic morphogenesis. *Neuron*, **29**, 229–242.

Poulopoulos, A., Aramuni, G., Meyer, G., Soykan, T., Hoon, M., Papadopoulos, T., Zhang, M., Paarmann, I., Fuchs, C., Harvey, K., Jedlicka, P., Schwarzacher, S.W., Betz, H., Harvey, R.J., Brose, N., Zhang, W. & Varoqueaux, F. (2009) Neuroligin 2 drives postsynaptic assembly at perisomatic inhibitory synapses through gephyrin and collybistin. *Neuron*, **63**, 628–642.

Reid, T., Bathoorn, A., Ahmadian, M.R. & Collard, J.G. (1999) Identification and characterization of hPEM-2, a guanine nucleotide exchange factor specific for Cdc42. *J. Biol. Chem.*, **274**, 33587–33593.

Ridley, A.J. & Hall, A. (1992) The small GTP-binding protein rho regulates the assembly of focal adhesions and actin stress fibers in response to growth factors. *Cell*, **70**, 389–399.

Rossman, K.L., Worthylake, D.K., Snyder, J.T., Siderovski, D.P., Campbell, S.L. & Sondek, J. (2002) A crystallographic view of interactions between Dbs and Cdc42: PH domain-assisted guanine nucleotide exchange. *EMBO J.*, **21**, 1315–1326.

Rossman, K.L., Cheng, L., Mahon, G.M., Rojas, R.J., Snyder, J.T., Whitehead, I.P. & Sondek, J. (2003) Multifunctional roles for the PH domain of Dbs in regulating Rho GTPase activation. *J. Biol. Chem.*, **278**, 18393–18400.

Saiyed, T., Paarmann, I., Schmitt, B., Haeger, S., Sola, M., Schmalzing, G., Weissenhorn, W. & Betz, H. (2007) Molecular basis of gephyrin clustering at inhibitory synapses: role of G- and E-domain interactions. *J. Biol. Chem.*, **282**, 5625–5632.

Schiller, M.R., Blangy, A., Huang, J., Mains, R.E. & Eipper, B.A. (2005) Induction of lamellipodia by Kalirin does not require its guanine nucleotide exchange factor activity. *Exp. Cell Res.*, **307**, 402–417.

Schmidt, A. & Hall, A. (2002) Guanine nucleotide exchange factors for Rho GTPases: turning on the switch. *Genes Dev.*, **16**, 1587–1609.

Skowronek, K.R., Guo, F., Zheng, Y. & Nassar, N. (2004) The C-terminal basic tail of RhoG assists the guanine nucleotide exchange factor trio in binding to phospholipids. *J. Biol. Chem.*, **279**, 37895–37907.

Snyder, J.T., Worthylake, D.K., Rossman, K.L., Betts, L., Pruitt, W.M., Siderovski, D.P., Der, C.J. & Sondek, J. (2002) Structural basis for the selective activation of Rho GTPases by Dbl exchange factors. *Nat. Struct. Biol.*, **9**, 468–475.

Soykan, T., Poulopoulos, A., Papadopoulos, T., Betz, H., Brose, N. & Varoqueaux, F. (2009) A mechanistic model underlying inhibitory synapse assembly. *Soc. Neurosci. Abstr.* Program No., **422.14**.

Symons, M., Derry, J.M., Karlak, B., Jiang, S., Lemahieu, V., McCormick, F., Francke, U. & Abo, A. (1996) Wiskott-Aldrich syndrome protein, a novel effector for the GTPase CDC42Hs, is implicated in actin polymerization. *Cell*, **84**, 723–734.

Varoqueaux, F., Jamain, S. & Brose, N. (2004) Neuroligin 2 is exclusively localized to inhibitory synapses. *Eur. J. Cell Biol.*, **83**, 449–456.

Wonders, C. & Anderson, S.A. (2005) Cortical interneurons and their origins. *Neuroscientist*, **11**, 199–205.

Woolfrey, K.M., Srivastava, D.P., Photowala, H., Yamashita, M., Barbolina, M.V., Cahill, M.E., Xie, Z., Jones, K.A., Quilliam, L.A., Prakriya, M. & Penzes, P. (2009) Epac2 induces synapse remodeling and depression and its disease-associated forms alter spines. *Nat. Neurosci.*, **12**, 1275–1284.

Worthylake, D.K., Rossman, K.L. & Sondek, J. (2000) Crystal structure of Rac1 in complex with the guanine nucleotide exchange region of Tiam1. *Nature*, **408**, 682–688.

Wu, X., Quondamatteo, F., Lefever, T., Czuchra, A., Meyer, H., Chrostek, A., Paus, R., Langbein, L. & Brakebusch, C. (2006) Cdc42 controls progenitor cell differentiation and beta-catenin turnover in skin. *Genes Dev.*, **20**, 571–585.

Xiang, S., Kim, E.Y., Connelly, J.J., Nassar, N., Kirsch, J., Winking, J., Schwarz, G. & Schindelin, H. (2006) The crystal structure of Cdc42 in complex with collybistin II, a gephyrin-interacting guanine nucleotide exchange factor. *J. Mol. Biol.*, **359**, 35–46.

Yoshizawa, M., Sone, M., Matsuo, N., Nagase, T., Ohara, O., Nabeshima, Y. & Hoshino, M. (2003) Dynamic and coordinated expression profile of dbl-family guanine nucleotide exchange factors in the developing mouse brain. *Gene Expr. Patterns*, **3**, 375–381.

Yu, J.W., Mendrola, J.M., Audhya, A., Singh, S., Keleti, D., DeWald, D.B., Murray, D., Emr, S.D. & Lemmon, M.A. (2004) Genome-wide analysis of membrane targeting by S. cerevisiae pleckstrin homology domains. *Mol. Cell*, **13**, 677–688.

Zhu, K., Debreceni, B., Li, R. & Zheng, Y. (2000) Identification of Rho GTPase-dependent sites in the Dbl homology domain of oncogenic Dbl that are required for transformation. *J. Biol. Chem.*, **275**, 25993–26001.